

# Design and Implementation of a 94 GHz CMOS Down-Conversion Mixer for Image Radar Sensors

Yo-Sheng Lin, Chien-Chin Wang, Guo-Hao Li, and Jay-Min Liu

Department of Electrical Engineering,  
National Chi Nan University,  
Puli, Taiwan, ROC

Emails: stephenlin@ncnu.edu.tw, s99323901@ncnu.edu.tw, s101323507@ncnu.edu.tw, s102323518@ncnu.edu.tw

**Abstract**— A 94 GHz down-conversion mixer for image radar sensors using standard 90 nm CMOS technology is reported. The down-conversion mixer comprises a double-balanced Gilbert cell with peaking inductors between RF transconductance stage and LO switching transistors for Conversion Gain (CG) enhancement and Noise Figure (NF) suppression, a Marchand balun for converting the single RF input signals to differential signals, another Marchand balun for converting the single LO input signals to differential signals, and an IF amplifier. The mixer consumes 22.5 mW and achieves excellent RF-port input reflection coefficient of  $-7.1\sim -35.9$  dB for frequencies of 82.6~96 GHz, and LO-port input reflection coefficient of  $-10\sim -35.9$  dB for frequencies of 88.2~110 GHz. In addition, the mixer achieves CG of  $-3.4\sim -6.4$  dB for frequencies of 85~97 GHz (the corresponding 3-dB CG bandwidth is 12 GHz) and LO-RF isolation of 41~47.2 dB for frequencies of 90~100 GHz, one of the best CG and LO-RF isolation results ever reported for a down-conversion mixer with operation frequency around 94 GHz. Furthermore, the mixer achieves an excellent input third-order intercept point (IIP3) of  $-3$  dBm at 94 GHz. These results demonstrate the proposed down-conversion mixer architecture is promising for 94 GHz image radar sensors.

**Keywords**— CMOS; down-conversion mixer; conversion gain; noise figure; LO-RF isolation

## I. INTRODUCTION

Recently, several excellent GaAs down-conversion mixers for operation frequencies around 94 GHz have been reported [1]-[3]. For example, in [1], a 90~112 GHz image reject down-conversion mixer with an improved Lange coupler in 0.15  $\mu\text{m}$  GaAs PHEMT process is demonstrated. Though wide bandwidth of 22 GHz was achieved, its performances, such as CG of  $-10$  dB, LO-RF isolation of 30 dB, and chip area of 4  $\text{mm}^2$  are not good enough. In [2], a 90~97 GHz single balanced down-conversion mixer using a rat-race hybrid ring with five ports and two GaAs Schottky diodes is reported. Though wide bandwidth of 7 GHz was achieved, its conversion gain of  $-12.6$  is not satisfactory. In [3], a 94 GHz single balanced down-conversion mixer using branch line couplers in 0.1  $\mu\text{m}$  GaAs process is demonstrated. Similarly, its performances, such as CG of  $-14.7$  dB, LO-RF isolation of 34.2 dB, and chip area of 3.38  $\text{mm}^2$  are not good enough. In this work, to demonstrate that low power dissipation ( $< 25$  mW), high CG ( $> -5$  dB), excellent LO-RF isolation ( $> 40$  dB) and small chip

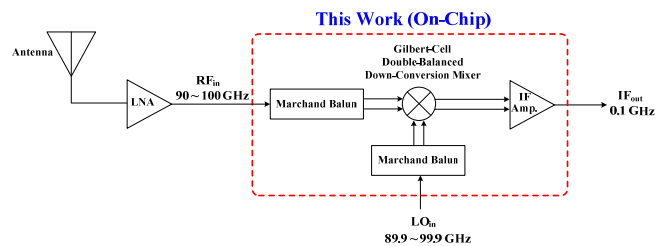


Figure 1. Block diagram of the proposed 94 GHz down-conversion mixer.

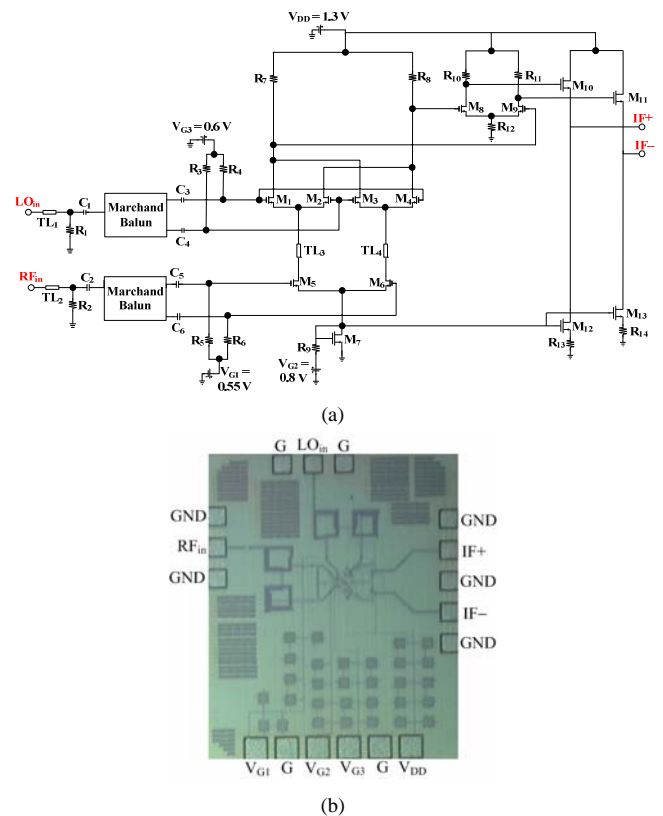


Figure 2. (a) Schematic, and (b) chip microphotograph of the 94 GHz CMOS down-conversion mixer.

area ( $< 1 \text{ mm}^2$ ) can be achieved simultaneously for a CMOS down-conversion mixer with operation frequency around 94GHz, we report a miniature low-power 94 GHz down-

conversion mixer with excellent CG, 3-dB bandwidth ( $\omega_{3dB}$ ) and port-to-port isolation properties using cost-effective standard 90 nm CMOS technology. In Section 2, circuit design is introduced. In Section 3, we demonstrate the measurement results and provide some discussions. Section 4 presents the conclusion.

## II. CIRCUIT DESIGN

The 94 GHz down-conversion mixer was designed and implemented in a standard 90 nm CMOS process provided by a commercial foundry. This technology offers 9 metal layers, named MT<sub>1</sub> to MT<sub>9</sub> from bottom to top. The thickness of MT<sub>9</sub> is 3.4  $\mu\text{m}$ , and that of MT<sub>8</sub>, MT<sub>7</sub>~MT<sub>2</sub> and MT<sub>1</sub> is 0.85  $\mu\text{m}$ , 0.31  $\mu\text{m}$  and 0.24  $\mu\text{m}$ , respectively. The interconnection lines as well as the microstrip-line (MSL) inductors were implemented with the 3.4- $\mu\text{m}$ -thick topmost metal to minimize the resistive loss. Figure 1 shows the block diagram of the proposed 94 GHz down-conversion mixer.

Figure 2(a) shows the schematic of the 94 GHz CMOS down-conversion mixer. The mixer comprises a double-balanced Gilbert cell, a miniature wideband Marchand balun for converting the single RF input signal to differential signal, another miniature wideband Marchand balun for converting the single LO input signal to differential signal, and an IF amplifier (which constitutes a resistive source-degeneration IF differential amplifier followed by a source-follower IF buffer amplifier). Note that the double-balanced Gilbert cell has peaking inductors between RF transconductance stage and LO switching transistors for CG improvement and NF suppression. With the addition of the tail current source comprising transistor M<sub>7</sub> and resistor R<sub>9</sub>, the RF transconductance stage operates as an elegant, yet robust differential pair. The current of the tail current source is also mirrored to the IF buffer amplifier constitutes transistors M<sub>10</sub>~M<sub>13</sub> and resistors R<sub>12</sub>~R<sub>13</sub>. The driving current of the IF buffer amplifier can be tuned by varying the resistance of resistors R<sub>12</sub>~R<sub>13</sub>. The chip micrograph of the mixer is shown in Figure 2(b). The chip area is only 0.69×0.84 mm<sup>2</sup> excluding the test pads.

Figure 3(a) shows the schematic diagram of the Marchand balun used in the mixer. It is designed based on the "lumped-element" Marchand balun structure proposed in [4]. Such a balun structure is advantageous in terms of its excellent amplitude/phase match and broadband response compared with the traditional single-to-differential transformers. Instead of the area-consumed straight-line or U-shaped MSL structures, the miniature spiral coil MSL structure, i.e. with the patterned MT<sub>1</sub> ground plane (with MT<sub>1</sub> density of about 56%) underneath and around the MSL structure, as shown in Figure 3(b), is adopted to implement the needed inductor elements in the baluns. The metal width and space are 4  $\mu\text{m}$  and 2  $\mu\text{m}$ , respectively. The balun consists of an unbalanced input (Port 1) with 50  $\Omega$  terminal impedance, an open terminal (O.C.), two short terminals (GND) and two balanced outputs (Port 2 and Port 3)

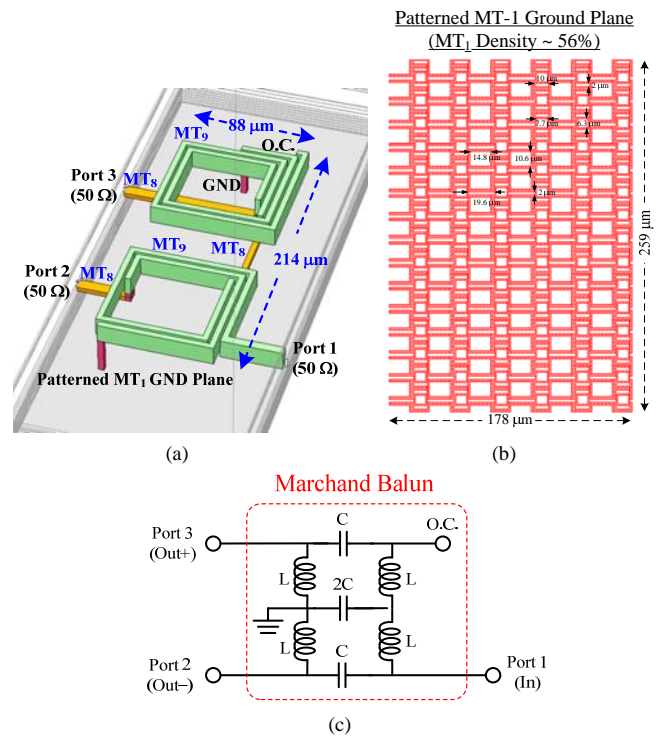


Figure 3. (a) Schematic diagram, (b) metal-1 patterned ground plane, and (c) lump-element equivalent circuit of the proposed 94-GHz-band Marchand balun.

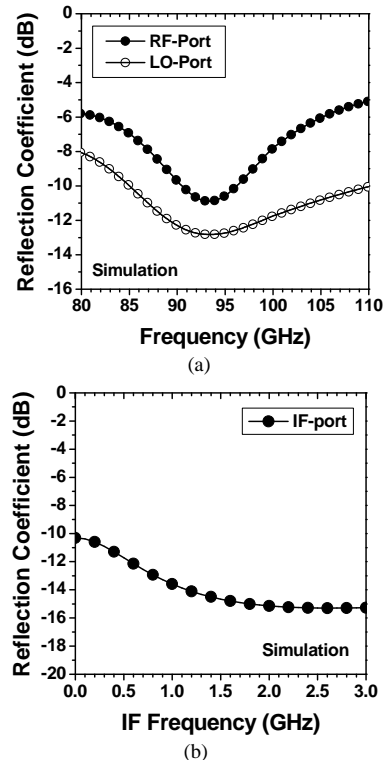


Figure 4. Simulated input reflection coefficients of the down-conversion mixer (a) at RF-port and LO-port and (b) at IF-port.

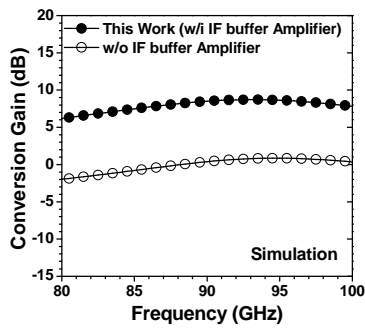


Figure 5. Simulated CG versus frequency characteristics of the down-conversion mixer.

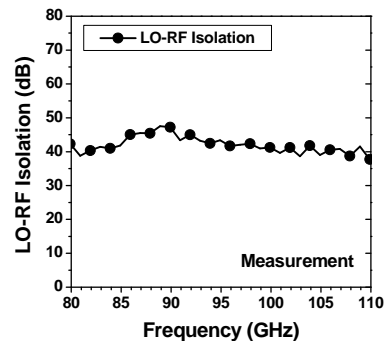
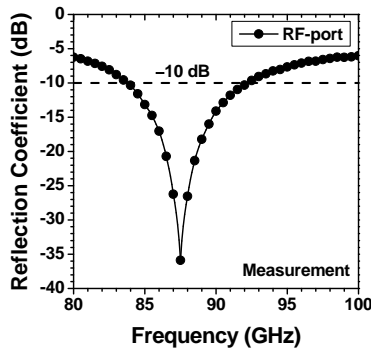
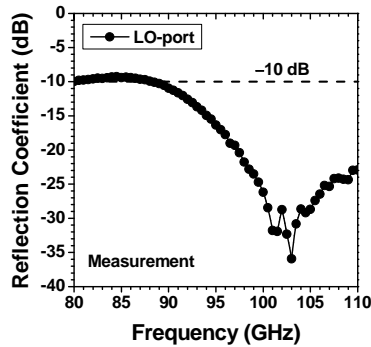


Figure 8. Measured LO-RF isolation versus frequency characteristics of the down-conversion mixer.



(a)



(b)

Figure 6. Measured (a) input reflection coefficients at RF-port ( $S_{11}$ ), and (b) input reflection coefficients at LO-port ( $S_{22}$ ) versus frequency characteristics of the down-conversion mixer.

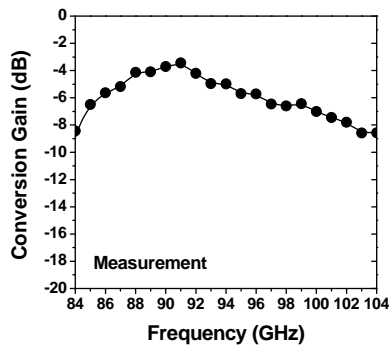


Figure 7. Measured CG versus RF frequency characteristics of the down-conversion mixer.

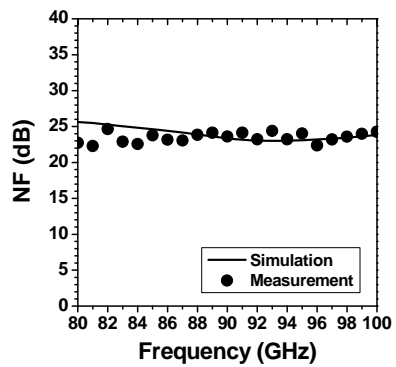


Figure 9. Measured and simulated NF versus frequency characteristics of the down-conversion mixer.

with  $50 \Omega$  terminal impedance. Note that the coils of the balun are implemented by the  $3.4\text{-}\mu\text{m}$ -thick topmost metal ( $MT_9$ ) to minimize the resistive loss. Only the underpass interconnection lines are realized by  $MT_8$ .

Figure 3(c) shows the lump-element balun equivalent circuit [4]. The spiral coil couple-line is modeled by the lump inductor  $L$ , and the capacitor  $C$  models the coupling capacitance effect produced from the spiral coil couple-line. That is, the capacitors are realized as the parasitic components of the inductors. Port 1 is the unbalanced RF input port (or LO output port), and port 2 and port 3 are the balanced RF+ and RF- output port (or LO+ and LO- input port), respectively. In a network, this lump-element balun can be regarded as an out-of-phase power splitter, including a parallel-connected high-pass filter and a band-pass filter. The signals through the output ports of the ideal balun have equal power but are  $180^\circ$  out-of-phase; all ports (except the O.C. port) have an input impedance of  $50 \Omega$  (i.e.  $Z_0$ ).

Figure 4(a) shows the simulated input reflection coefficients at RF-port ( $S_{11}$ ) versus RF frequency characteristics of the down-conversion mixer. The mixer achieves  $S_{11}$  of  $-10.8 \text{ dB}$  at  $94 \text{ GHz}$ , and  $S_{11}$  smaller than  $-10 \text{ dB}$  for RF frequencies of  $90.5\text{--}96.2 \text{ GHz}$ . That is, the simulated  $-10 \text{ dB}$  input matching bandwidth at RF-port is  $5.7 \text{ GHz}$ . What is also shown in Figure 4(a) is the simulated input

TABLE I. SUMMARY OF THE IMPLEMENTED 94 GHz CMOS DOWN-CONVERSION MIXER, AND RECENTLY REPORTED STATE-OF-THE-ART DOWN-CONVERSION MIXERS WITH OPERATION FREQUENCY AROUND 94 GHz.

References	Topology	RF Frequency (GHz)	IF Frequency (GHz)	CG (dB)	LO-RF Isolation (dB)	Power (mW)	Chip Area (mm <sup>2</sup> )	Technology (nm)	f <sub>T</sub> /f <sub>max</sub> (GHz)
This Work	Gilbert-Cell with Source-Follower Output Buffer	94	0.1	-3.4	47.5	22.5	0.58	CMOS (90)	152/157
[1] (2011 MTT-S)	Image-Reject with Improved Lange Coupler	94	6	-10	30	NA	4	GaAs PHEMT (150)	NA
[2] (2010 ICMMT)	Rat-Race Hybrid-Ring with Five Ports and Two Diodes	94	0.5	-12.6	NA	NA	NA	GaAs Schottky Diode	NA
[3] (2012 GSMM)	Single-Balanced Using Branch Line Couplers	94	0.325	-14.7	34.2	NA	3.38	GaAs MHEMT (100)	189/334

reflection coefficients at LO-port ( $S_{22}$ ) versus LO frequency characteristics of the down-conversion mixer. The mixer achieves  $S_{22}$  of -12.8 dB at 94 GHz, and  $S_{22}$  smaller than -10 dB for RF frequencies of 85~110.2 GHz. That is, the simulated -10 dB input matching bandwidth at LO-port is 25.2 GHz.

Figure 4(b) shows the simulated input reflection coefficients at IF-port ( $S_{33}$ ) versus IF frequency characteristics of the down-conversion mixer. The mixer achieves excellent  $S_{33}$  of -10.3~ -15.3 dB for IF frequencies of 0~3 GHz.

Figure 5 shows the simulated CG versus frequency characteristics of the mixer both with and without the IF amplifier. RF input power is -40 dBm and LO input power is 4 dBm. The mixer achieves CG of 8.7 dB at 94 GHz, and CG of 7.82~8.72 dB for frequencies of 90~100 GHz, one of the best CG results ever reported for a down-conversion mixer with operation frequency around 94 GHz. The corresponding 3-dB bandwidth is larger than 21.8 GHz (78.2~100 GHz). In the case without the IF amplifier, the mixer achieves inferior CG of 0.84 dB at 94 GHz, and CG of 0.36~0.85 dB for frequencies of 90~100 GHz. The corresponding 3-dB bandwidth is larger than 21.1 GHz (78.9~100 GHz).

### III. MEASUREMENT RESULTS AND DISCUSSIONS

On-wafer measurements were performed by an Agilent's 110 GHz RFIC measurement system. The down-conversion mixer is biased in the condition of  $V_{DD} = 1.3$  V and  $I_{DD} = 17.3$  mA. That is, the simulated power consumption of the mixer is 22.5 mW. Figure 6(a) shows the measured  $S_{11}$ . The mixer achieves excellent  $S_{11}$  of -8.3 dB at 94 GHz, and  $S_{11}$  of -7.1~ -35.9 dB for frequencies of 82.6~96 GHz. Figure 6(b) shows the measured  $S_{22}$ . The mixer achieves excellent  $S_{22}$  of -14.9 dB at 94 GHz, and  $S_{22}$  of -10~ -35.9 dB for frequencies of 88.2~110 GHz. That is, the measured -10 dB LO input matching bandwidth is larger than 21.8 GHz.

Figure 7 shows the measured CG versus frequency characteristics of the down-conversion mixer. The mixer achieves maximum CG of -3.4 dB at 91 GHz and CG of -3.4~ -6.4 dB for frequencies of 85~97 GHz, one of the best CG results ever reported for a down-conversion mixer with

operation frequency around 94 GHz. The corresponding 3-dB bandwidth is 12 GHz (85~97 GHz).

Figure 8 shows the measured LO-RF isolation versus frequency characteristics of the mixer. The mixer achieves LO-RF isolation of 41~47.2 dB for frequencies of 90~100 GHz, one of the best LO-RF isolation results ever reported for a down-conversion mixer with operation frequency around 94 GHz. Furthermore, the mixer achieves an excellent IIP3 of -3 dBm at 94 GHz (not shown here).

Figure 9 shows the measured and simulated NF versus frequency characteristics of the down-conversion mixer. As can be seen, the measured results conform with the simulated ones well. The mixer achieves NF of 23.2 dB at 94 GHz, and NF of 22.4~24.4 dB for frequencies of 90~100 GHz.

Table I is a summary of the implemented 90~100 GHz CMOS down-conversion mixer, and recently reported state-of-the-art down-conversion mixers with operation frequency around 94 GHz. Compared with the 90~112 GHz image reject down-conversion mixer in [1], the proposed mixer exhibits better CG and LO-RF isolation, and smaller chip area. Compared with the 90~97 GHz single balanced GaAs down-conversion mixer in [2], the proposed mixer exhibits better CG. Compared with the 94 GHz single balanced GaAs down-conversion mixer in [3], the proposed mixer exhibits better CG and LO-RF isolation, and smaller chip area. These results indicate that our proposed down-conversion mixer is suitable for W-band transceiver systems.

### IV. CONCLUSION

In this work, we reported a 90~100 GHz CMOS down-conversion mixer comprises a double-balanced Gilbert-cell, a miniature wideband RF Marchand balun, a miniature wideband LO Marchand balun, and an IF amplifier. The mixer consumes 22.5 mW and achieves excellent CG of -3.4~ -6.4 dB for frequencies of 85~97 GHz, that is, the corresponding 3-dB bandwidth of RF is 12 GHz. Moreover, excellent LO-RF isolation is also achieved. These results highlight the potential application of the proposed down-conversion mixer architecture in 94 GHz and even higher frequency communication systems.

## REFERENCES

- [1] Y. C. Wu, S. K. Lin, C. C. Chiong, Z. M. Tsai, and H. Wang, "A W-Band Image Reject Mixer for Astronomical Observation System," IEEE MTT-S International Microwave Symposium, 2011, pp. 1-4.
- [2] W. Zhao, Y. Zhang, and M. Z. Zhan, "Design and Performance of a W-Band Microstrip Rat-Race Balanced Mixer," International Conference on Microwave and Millimeter Wave Technology, 2010, pp. 713-716.
- [3] S. J. Lee, T. J. Baek, M. Han, S. G. Choi, D. S. Ko, and J. K. Rhee, "94 GHz MMIC Single-Balanced Mixer for FMCW Radar Sensor Application," Global Symposium on Millimeter Waves, 2012, pp. 351-354.
- [4] P. C. Yeh, W. C. Liu, and H. K. Chiou, "Compact 28-GHz Subharmonically Pumped Resistive Mixer MMIC Using a Lumped-Element High-Pass/Band-Pass Balun," IEEE Microwave and Wireless Components Letters, vol. 15, no. 2, Feb. 2005, pp. 62-64.